






Article

A Molecular Test for Quantifying Functional Notch Signaling Pathway Activity in Human Cancer

Kirsten Canté-Barrett ^{1,†,‡} , Laurent Holtzer ^{2,†}, Henk van Ooijen ³ , Rico Hagelaar ¹,
Valentina Cordo' ¹ , Wim Verhaegh ³ , Anja van de Stolpe ^{2,§} and Jules P. P. Meijerink ^{1,*} 

¹ Princess Máxima Center for Pediatric Oncology, 3584 CS Utrecht, The Netherlands; K.Cante@prinsesmaximacentrum.nl (K.C.-B.); R.Hagelaar@prinsesmaximacentrum.nl (R.H.); v.cordo@prinsesmaximacentrum.nl (V.C.)

² Philips Molecular Pathway Dx, Royal Philips, 5656 AE Eindhoven, The Netherlands; laurent.holtzer@philips.com (L.H.); anja.van.de.stolpe@philips.com (A.v.d.S.)

³ Philips Research, Royal Philips, 5656 AE Eindhoven, The Netherlands; henk.van.ooijen@philips.com (H.v.O.); wim.verhaegh@philips.com (W.V.)

* Correspondence: j.meijerink@prinsesmaximacentrum.nl; Tel.: +31-6-15064275

† These authors share equal contribution.

‡ Present address: Department of Immunology, Leiden University Medical Center, 2333ZA Leiden, The Netherlands.

§ These authors share equal senior authorship.

Received: 24 September 2020; Accepted: 18 October 2020; Published: 27 October 2020



Simple Summary: The Notch signal transduction pathway is important for various physiological processes, including immune responses, and plays a role in many diseases, for example cancer. We have developed a new assay to quantitatively measure Notch pathway activity, and we validated it using data from various human cancer cell lines. The assay can be applied across different cell types, and offers numerous possibilities to explore the contribution of the Notch pathway to tumor formation and the stratification of cancer patients. We assessed Notch pathway activity in a cohort of T cell acute lymphoblastic leukemia (T-ALL) patient samples, and found that the pathway activity score more accurately reflects Notch pathway activity than a prediction on the basis of *NOTCH1* mutations alone. Finally, we found that patients with low Notch pathway activity had a significantly shorter event-free survival compared to patients who had T-ALL cells with higher activity.

Abstract: Background: The Notch signal transduction pathway is pivotal for various physiological processes, including immune responses, and has been implicated in the pathogenesis of many diseases. The effectiveness of various targeted Notch pathway inhibitors may vary due to variabilities in Notch pathway activity among individual patients. The quantitative measurement of Notch pathway activity is therefore essential to identify patients who could benefit from targeted treatment. Methods: We here describe a new assay that infers a quantitative Notch pathway activity score from the mRNA levels of generally conserved direct NOTCH target genes. Following the calibration and biological validation of our Notch pathway activity model over a wide spectrum of human cancer types, we assessed Notch pathway activity in a cohort of T-ALL patient samples and related it to biological and clinical parameters, including outcome. Results: We developed an assay using 18 select direct target genes and high-grade serous ovarian cancer for calibration. For validation, seven independent human datasets (mostly cancer series) were used to quantify Notch activity in agreement with expectations. For T-ALL, the median Notch pathway activity was highest for samples with strong NOTCH1-activating mutations, and T-ALL patients of the TLX subtype generally had the highest levels of Notch pathway activity. We observed a significant relationship between ICN1 levels and the absence/presence of NOTCH1-activating mutations with Notch pathway activity scores. Patients with the lowest Notch activity scores had the shortest event-free survival compared to other patients. Conclusions: High Notch pathway activity was not limited to T-ALL samples harboring

strong NOTCH1 mutations, including juxtamembrane domain mutations or hetero-dimerization combined with PEST-domain or FBXW7 mutations, indicating that additional mechanisms may activate Notch signaling. The measured Notch pathway activity was related to intracellular NOTCH levels, indicating that the pathway activity score more accurately reflects Notch pathway activity than when it is predicted on the basis of NOTCH1 mutations. Importantly, patients with low Notch pathway activity had a significantly shorter event-free survival compared to patients showing higher activity.

Keywords: Notch pathway activity; NOTCH1 mutation; T cell acute lymphoblastic leukemia

1. Introduction

An increasing number of precision drugs are becoming available for clinical medicine, and many more are in development. These targeted drugs are intended for personalized medicine and aim at targeting the pathophysiological defects underlying specific diseases in individual patients. For cancer, but also for many other diseases including auto-immune or immune-mediated diseases, patient samples may display a similar histopathology, while significant pathophysiological variations can be found at the cellular level [1,2]. Such variations may be the reason that only a portion of all patients with a specific disease responds to a targeted drug. Matching the right drug to the right patient has therefore become an increasingly important issue. However, developing a diagnostic approach to reliably predict therapy responses has proven difficult. The prime example is oncology, wherein efforts in predicting patient responses to targeted drugs based on cancer genome mutations have generally been disappointing, despite exceptions in select cases [3–7]. To improve clinical decision-making regarding targeted treatment, and therefore to improve clinical outcomes, assays are needed that accurately characterize and quantify the underlying pathophysiological processes in individual patient samples [1,8–17]. Cellular signal transduction pathways are evolutionarily conserved, and control fundamental cellular processes such as cell division, differentiation, migration and metabolism [1,18–20]. They include nuclear receptor pathways (e.g., androgen and estrogen receptor pathways), developmental pathways (Wnt, Hedgehog, TGF β and Notch), the highly complex growth factor- and cytokine-regulated signaling pathway network (including JAK-STAT, PI3K-AKT-mTOR and MAPK pathways), and the inflammatory NF κ B pathway [18,21]. The measurement of the functional activity of these pathways in tumor biopsies from individual patients is expected to improve the prediction of therapy response. We have previously described a novel approach to quantitatively measure the activity levels of individual signal transduction pathways in various cell and tissue types [22–25]. In addition to the development of assays to measure the activity of the estrogen and androgen receptor pathways, the PI3K, JAK-STAT3, Wnt, Hedgehog, TGF β , NF κ B and JAK-STAT1/2 pathways, we now report the development and biological validation of a quantitative Notch pathway activity assay. The human Notch pathway is an evolutionarily highly conserved developmental signaling pathway, activated by the interaction of one of four NOTCH transmembrane receptors with Jagged or Delta-like Canonical Notch ligands on neighboring cells [16]. Upon ligand binding, the receptor is cleaved by two consecutive protease steps that include an ADAM (a disintegrin and metalloproteinase) protease and the gamma-secretase complex. The resulting cleaved intracellular NOTCH (ICN) migrates to the nucleus, where it forms a transcription factor complex with DNA binding factor RBPJ (recombination signal binding protein for immunoglobulin kappa J region) and coactivators of the MAML (Mastermind-like) family, and activates the transcription of its target genes. The Notch pathway plays a role in multiple diseases, including T-cell acute lymphoblastic leukemia (T-ALL) [16,26]. Notch pathway inhibitors have been developed for multiple potential clinical applications, but their use has generally been associated with severe side effects [27–32]. In addition, NOTCH inducers have been developed, e.g., for small cell lung cancer [33].

A major clinical challenge is to minimize side effects and identify patients who benefit from Notch pathway-modifying drugs.

To illustrate the potential utility of the Notch pathway assay for clinical decision-making, a Notch pathway activity analysis was performed in a large cohort of diagnostic samples from pediatric T-ALL patients with known genetic backgrounds and mutation statuses. Activating mutations in the NOTCH1 pathway, including mutations in *NOTCH1* and/or *FBXW7* (which encodes for a ubiquitin ligase involved in the degradation of active intracellular NOTCH1 (ICN1)), are found in approximately 60% of T-ALL patients [34,35]. Publications on patient outcomes in T-ALL report different prognostic significances for *NOTCH1*-activating mutations alone [36]. We present evidence that patients with active Notch pathway signaling have a more favorable long-term outcome when on high-intensity combination treatment protocols [37–39].

2. Results

2.1. Development of the Notch pathway Assay and Selection of NOTCH Target Genes

For the development of the Notch pathway assay, we selected high evidence direct target genes of NOTCH. This selection was based on (i) the presence of minimally one binding element in the promoter region, (ii) the functionality of these binding elements that have been assessed, for instance, by gene promoter-reporter studies, (iii) the binding of ICN to the respective response/enhancer element using ChIP and/or Electrophoretic Mobility Shift Assay, (iv) their differential expression upon pathway activation and/or inhibition, and (v) the consistency of evidence as reported by multiple research groups for multiple cell/tissue types. Based on such accumulated experimental evidence as described before [22–24], we selected 18 direct target genes, *CD44*, *DTX1*, *EPHB3*, *HES1*, *HES4*, *HES5*, *HES7*, *HEY1*, *HEY2*, *HEYL*, *MYC*, *NFKB2*, *NOX1*, *NRARP*, *PBX1*, *PIN1*, *PLXND1* and *SOX9* (Table S1) [40–82]. This number is sufficient for the robust and sensitive prediction of the pathway activity while comprising only high evidence target genes that enable maximal specificity over multiple cell types.

2.2. Calibration and Validation of the Notch Pathway Activity Assay

We calibrated the Notch pathway assay using data from high-grade serous (HGS) ovarian cancer samples with high Notch pathway activity, and normal ovarian tissue samples with low Notch pathway activity (Figure 1A). While in healthy ovarian tissue samples the Notch pathway is inactive, HGS ovarian cancer is associated with an active Notch pathway and activating *NOTCH3* gene mutations or amplifications in about two third of the patients [83–86]. Following the freezing of the Notch pathway model, it was validated on various independent datasets from cells of different tissue origins with Notch pathway-activated or gamma-secretase inhibited conditions, including cell types from ectodermal (neuroblastoma) and endodermal (lung cancer cells) origins, in contrast to the mesodermal origin of the ovarian cancer samples the model had been calibrated on (Figure 1B–H). Two independent clones of a neuroblastoma cell line transfected with ICN3 showed a rapid and persistent quantitative increase in Notch pathway activity score, starting within 4 h and reaching a plateau activity at 12 h after transfection (Figure 1B). In leukemia, the AF1Q-MLLT11 fusion protein confers sensitivity to ligand-induced Notch pathway signaling [87,88]. Hematopoietic progenitor cells (CD34⁺CD45RA⁻Lin⁻) from umbilical cord blood were transduced with the A2M mutant version of this fusion product that sequesters it in the nucleus. Following a three-day exposure to immobilized NOTCH ligand Delta1ext-IgG at two different dose levels, high Notch pathway activity scores were measured for both mock and A2M transduced cells (Figure 1C). As expected, the Notch pathway activity scores were higher for A2M-transduced cells than control cells. This result provides additional evidence for the ability of the Notch pathway assay to quantify small differences in Notch pathway activity. In other experimental designs in which Notch pathway activity was inhibited by exposure to gamma-secretase inhibitors (GSIs), the robustness of the assay for various additional cell types was validated. A549 lung cancer cells exposed to the GSI RO4929097 for 6 or 24 h scored a significantly

lower Notch pathway activity than control A549 cells (Figure 1D). Similar findings were found for the GSI-exposed Mantle B-cell lymphoma cell line SP-49 and the NOTCH mutant Rec-1 line [89] (Figure 1E), and for the T-cell lymphoma and leukemia cell lines CUTLL1 and MOLT4 (Figure 1F,G). In CUTLL1 cells, the wash-out of the GSI resulted in the reactivation of the Notch pathway, which was accurately quantified (Figure 1H). Furthermore, a dominant-negative form of the NOTCH cofactor MAML1 (DNMAML1) synergized with GSI and resulted in the lowest Notch pathway activity score. Interestingly, in this study the removal of GSI was performed both in the absence and presence of the protein translation inhibitor cycloheximide, so as to exclude any feedback or secondary effects from NOTCH-induced gene products. The measured Notch pathway activity scores were independent of protein translation, confirming that all genes that are part of the computational Notch pathway model are indeed direct target genes (Figure S1). In summary, these results demonstrate that the ovarian cancer-calibrated Notch pathway assay can be used to measure Notch pathway activity levels in T-cells, while the limited results available on other cell types suggest that the assay may also be usable in cell types of endodermal and ectodermal origin.

2.3. Notch Pathway Activity in Pediatric T-ALL Patient Samples

Following biological validation of the Notch pathway assay, we measured the Notch pathway activity scores in diagnostic samples from 117 pediatric T-ALL patients. This dataset has been previously used to distinguish four main T-ALL subgroups (ETP-ALL/immature, TLX, Proliferative and TALLMO) based on their differential gene expression profiles that strongly correlate with unique oncogenic rearrangements [98]. Notch pathway activity scores ranged from -8.59 to 7.45 on the linear \log_2 odds scale. To investigate these scores in relation to the presence of specific types of Notch pathway-activating mutations, we categorized NOTCH1 mutations into weak or strong activating mutations, as done before [35,99,100]. Weak NOTCH1 activating mutations are considered mutations in the NOTCH1 heterodimerization domain (HD) or PEST domain, or inactivating mutations in *FBXW7*. Strong NOTCH1-activating mutations are mutations in the juxtamembrane domain, or HD-mutations combined with PEST domain or *FBXW7* mutations. Based on this division, the median Notch pathway activity score was lowest for the patient samples without NOTCH-activating mutations, and highest for the samples with strong NOTCH1-activating mutations ($p < 0.001$; Figure 2A). Still, there is considerable overlap in activity scores among these groups. To investigate the potential effect of differences in genetic background among patients, we compared Notch pathway activity levels between the four T-ALL subtypes. The TLX subtype had the highest Notch pathway activity scores compared to the other subtypes, and included 10 out of 23 patient samples with strong NOTCH mutations (Figure 2B). Various TLX samples without, or with only weak, NOTCH-activating mutations also had high Notch pathway activity scores, further supporting the previous observation that alternative Notch pathway-activating mechanisms may exist. We then related the activity scores to intracellular NOTCH1 (ICN1) levels as measured using reverse-phase protein array for 62 patient samples [35]. We observed a significant relationship between ICN1 levels and the absence or presence of NOTCH1-activating mutations (Figure 2C), and between ICN1 levels and the Notch pathway activity scores (Figure 2D). The significance of the correlation between ICN1 levels and Notch pathway activity was mainly attributed to the strong NOTCH1-activating mutations, as the significance was lost for patient samples without, or with only weak, NOTCH1-activating mutations (Figure S2). This raised the question of whether those samples could harbor other Notch pathway-activating mechanisms. For this, we assessed NOTCH3 protein levels as an alternative Notch pathway-activating mechanism for various *NOTCH1*/*FBXW7* non-mutated T-ALL patient samples with low ICN1 levels but high Notch pathway activity scores. We did not find expression of NOTCH3 protein in these or other T-ALL samples tested. We then excluded the influence of bone marrow or peripheral blood origin of the T-ALL samples on the Notch pathway activity scores. Therefore, the incidental discrepancy between ICN and Notch pathway activity scores remains unclear. In conclusion, the results show that the Notch pathway assay

quantitatively measures Notch pathway activity not only in cell line systems, but also in a cohort of primary T-ALL patient samples.

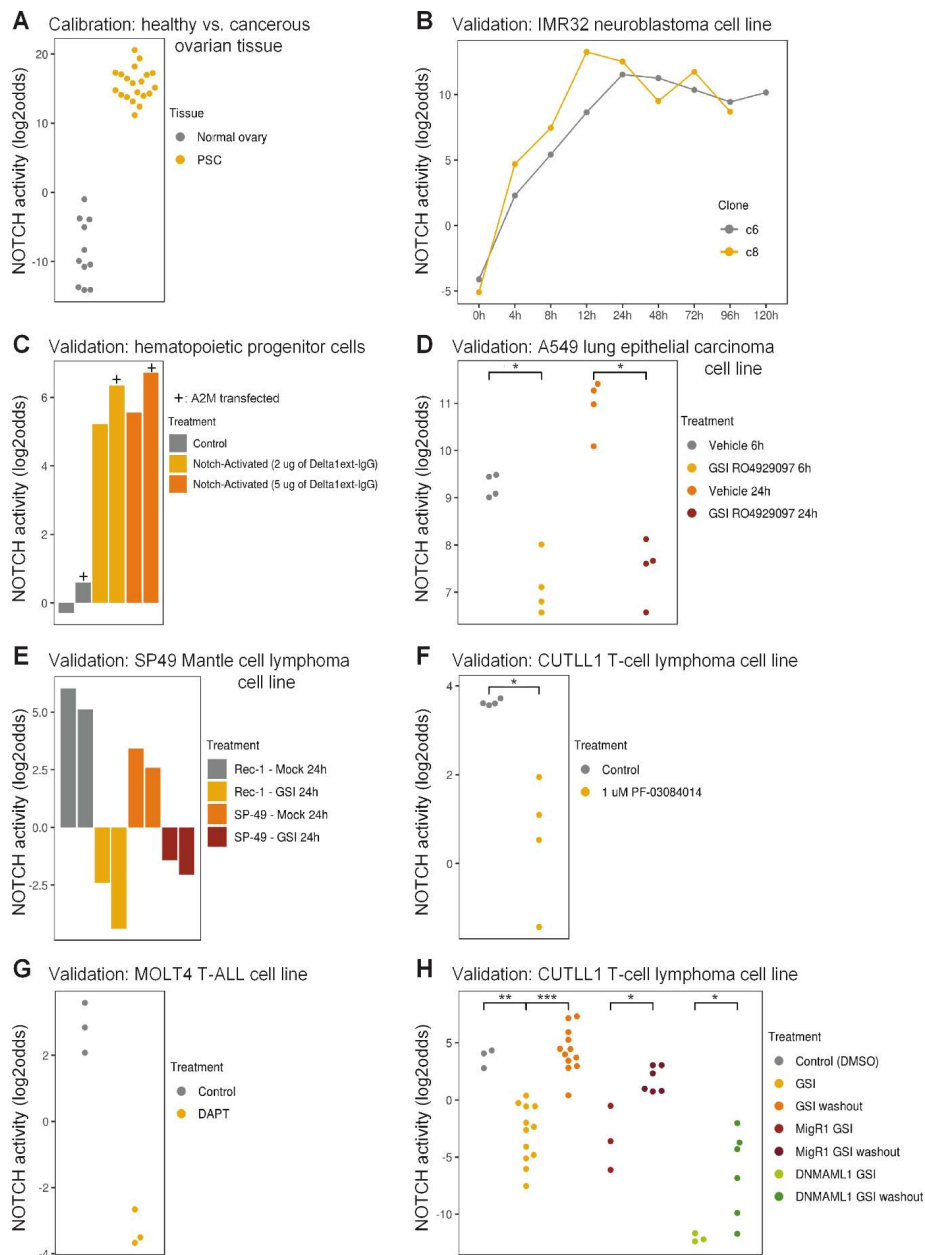


Figure 1. Calibration and biological validation of the Notch pathway model. **(A)** Calibration of the Notch pathway model. GSE7307, GSE18520 [90], GSE29450 [91], GSE36668 [92], normal ovarian tissue samples (inactive pathway); GSE2109, GSE9891 [93], high grade serous ovarian cancer samples (active pathway). **(B–G)** Validation of the model on independent GEO datasets from different cell lines. * $p < 0.05$, ** $p < 0.01$, *** $p < 0.001$. **(B)** GSE16477 [94]. Two clones (c6 and c8) of the IMR32 neuroblastoma cell line at different times (0–120 h) after induction of active intracellular NOTCH3. **(C)** GSE29524. A2M (+ symbol) or control vector-transfected CD34⁺CD45RA⁻Lin⁻ hematopoietic progenitor cells from umbilical cord blood were cultured for 72 h on a surface with 0, 2 or 5 μ g plastic-immobilized NOTCH ligand Delta1ext-IgG. A2M is a nuclear-trapped mutant of AF1q/MLL11. **(D)** GSE36176 [95]. A549 lung cancer cell lines subjected to vehicle control or gamma secretase inhibitor (GSI) RO4929097 for 6 or 24 h. **(E)** GSE34602 [89]. Rec-1 (containing an activating *NOTCH1* mutation) and SP49 Mantle cell lymphoma cell lines subjected to vehicle control or GSI compound E for 24 h.

(SP49 cells harbor an activating NOTCH4 rearrangement. (F) GSE33562 [96]. Duplicate samples of the CUTLL1 T-cell lymphoma cell line were subjected to vehicle control or the GSI PF-03084014 (1 μ M) for 48 h. (G) GSE6495 [97]. MOLT4 T-cell acute lymphoblastic leukemia cell line before and 48 h after addition of the GSI DAPT (5 μ M); three independent experiments. (H) GSE29544 [82]. CUTLL1 T-cell lymphoblastic lymphoma cells subjected to GSI compound E (1 μ M) for 3 days. From left to right: DMSO control; 3 grouped conditions: GSI without or with 2 or 4 h mock washout; 4 grouped conditions: GSI followed by 2 or 4 h GSI washout in the presence or absence of cycloheximide; GSI in presence of a control viral transcript MigR1; 2 grouped conditions: GSI in the presence of a control viral transcript MigR1 with 2 or 4 h washout; GSI in the presence of viral transcript DNMA1; 2 grouped conditions: GSI in the presence of viral transcript DNMA1 with 2 or 4 h washout. The activity score is calculated as log₂odds. Two-sided Wilcoxon signed-rank statistical tests were performed, *p*-values are indicated in the figures. In case fewer than 3 samples were needed for presentation, bar plots are used instead of dot plots.

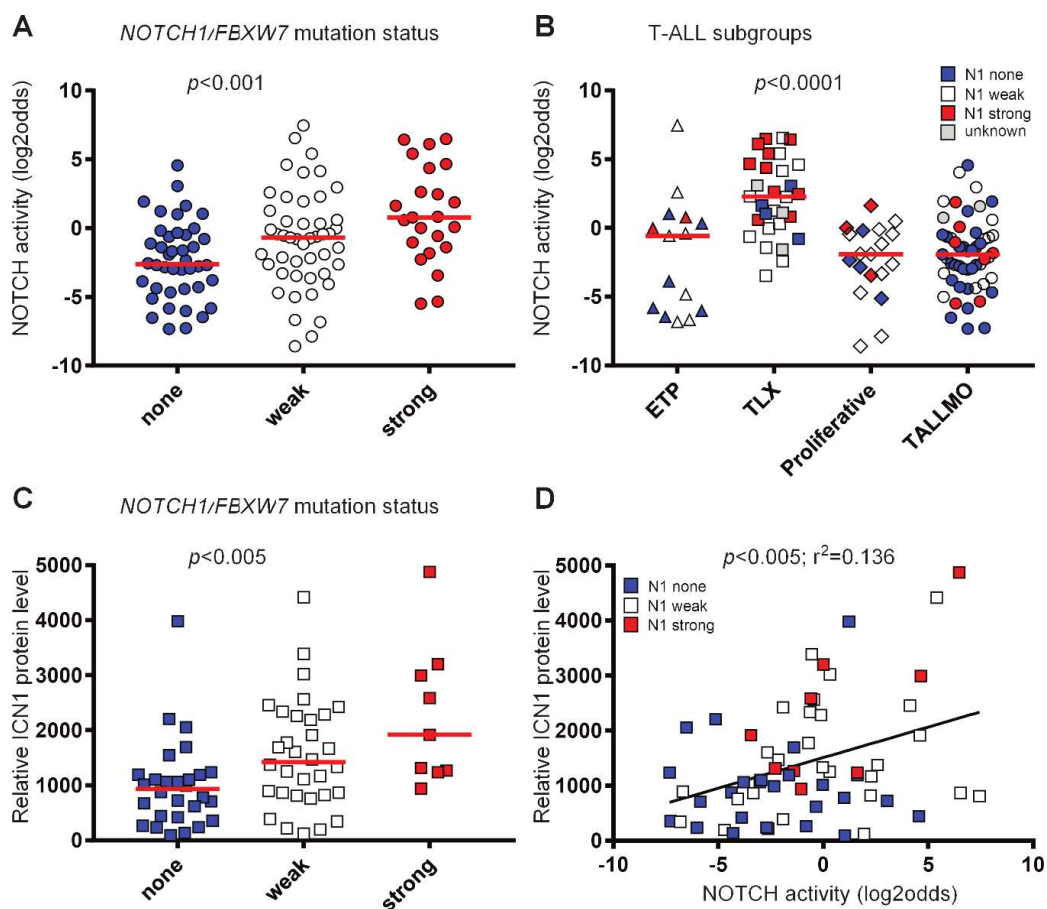


Figure 2. Notch pathway activity in T-ALL. (A–D) GSE26713 [98]. No NOTCH-activating mutations (blue symbols), weak NOTCH1-activating mutations (NOTCH1 heterodimerization domain, PEST domain or in FBXW7) (white symbols) and strong NOTCH1-activating mutations (juxtamembrane domain or more than one NOTCH1 activating mutation) (red symbols) are indicated. *p*-values are indicated. (A–C) Kruskal–Wallis statistical test. Medians are indicated by the red lines. (D) Linear regression test. (A) Notch pathway activity of T-ALL samples ($n = 112$) per *NOTCH1/FBXW7* mutation status group. (B) Notch pathway activity per T-ALL subgroup ($n = 117$). Five samples have an unknown *NOTCH1/FBXW7* mutation status (grey symbols). (C) Active intracellular NOTCH1 (ICN1) protein level measured in relative intensity units using reverse-phase protein array (RPPA), indicated per *NOTCH1/FBXW7* mutation status group ($n = 69$). (D) Correlation of active intracellular NOTCH1 (ICN1) protein level and Notch pathway activity ($n = 62$).

2.4. Notch Pathway Activity and T-ALL Patient Survival

The prognostic significance of NOTCH-activating mutations is not consistent in various patient studies [36]. Part of this may be due to the mechanisms, other than activating mutations in hotspots of *NOTCH1* or *FBXW7*, that activate Notch signaling in T-ALL patients, and which may explain the large overlap in the Notch pathway activity levels for T-ALL patients with and without *NOTCH1*/*FBXW7* mutations. In order to investigate outcomes in relation to Notch pathway activity, we divided the T-ALL patients into three groups based on their NOTCH activity scores: a group with the highest NOTCH activity scores (>75th percentile), a group with the lowest activity scores (<25th percentile) and a group with intermediate activity scores (between the 25th and 75th percentiles of activity scores). When assessing the event-free and relapse-free survival curves, we observed that the patients with the lowest activity scores had the shortest event-free survival compared to both of the other groups ($p < 0.05$), while relapse-free survival showed the same trend (Figure 3A,B).

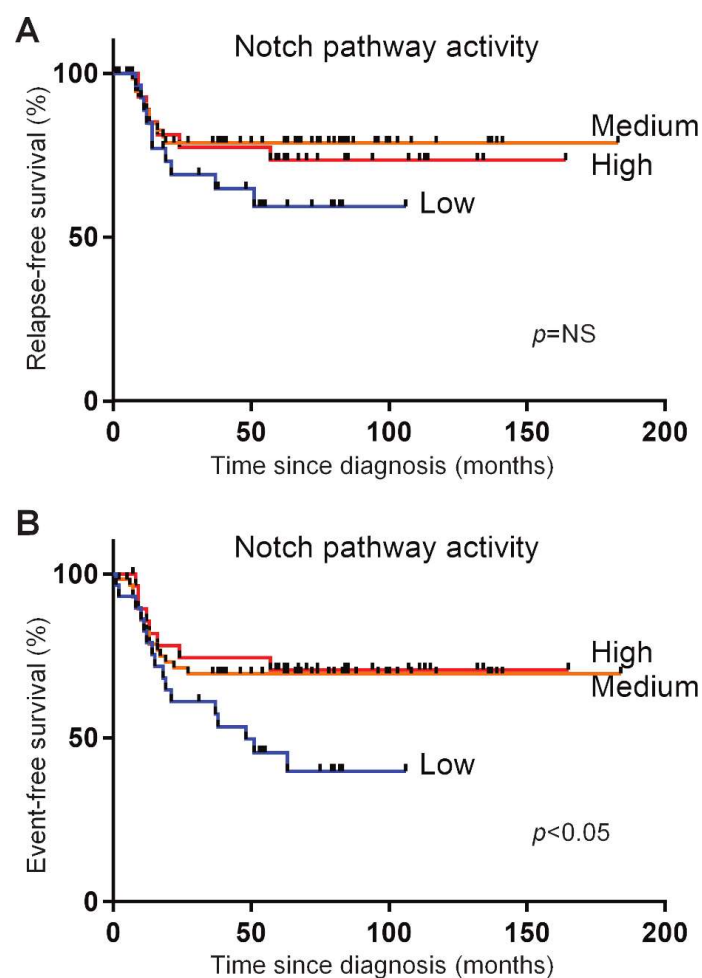


Figure 3. Relapse-free and event-free survival of T-ALL patients in three different Notch pathway activity groups. Three different Notch pathway activity groups were separated based on the lowest 25% Notch pathway activity (blue line), the highest 25% Notch pathway activity (red line), and the remaining 50%, termed the 'middle', Notch pathway activity (orange line). Relapse-free (A) and event-free (B) survival is plotted for the T-ALL pediatric patients treated on the DCOG ALL-7, -8 and -9 and COALL-97 protocols. $p = NS$ (not significant) (A) and $p < 0.05$ (B) (log-rank test). Events include relapse, non-responsiveness to induction or maintenance therapy, change of treatment or death due to infection, toxicity or other causes.

2.5. Relation between Notch Pathway Activity and PTEN Loss

The group with the lowest NOTCH activity scores contained patients that lacked either PTEN protein and/or had inactivating mutations or deletions in *PTEN*. We found an increased percentage of patients (11 out of 29, 38%) with functional PTEN loss in the group with the lowest Notch pathway activity, whereas only 12 out of the 84 patients (14%) with intermediate and high Notch pathway activity scores had functional PTEN loss ($p = 0.006$, Pearson Chi-Square, 2-sided).

3. Discussion

We have developed an assay to measure Notch pathway activity, consisting of a Bayesian network computational model which calculates a pathway activity score based on target gene expression levels. The set of NOTCH target genes was selected based on experimental evidence, irrespective of cell type or gene function [22–24]. The computational model was successfully validated on a variety of samples from different cell types with known Notch pathway activity, i.e., brain, lung, hematopoietic stem cells, and T-ALL cell lines. This suggests that the assay can be used on multiple different cell types without model recalibration, even across cell types originating from different embryonic germ layers. This is to a large extent enabled by the selection of high evidence *direct* transcriptional target genes of the NOTCH transcription factor family (e.g., NOTCH1, NOTCH2, NOTCH3), eliminating cell type-specific influences on target gene expression as much as possible. In addition, the Bayesian network model is well suited to handling variations in input data, which presents a crucial advantage when analyzing patient samples that are intrinsically highly variable in gene expression regulation [22]. Other RNA-based pathway analysis tools are available, mainly for biomarker discovery applications, and differences have been discussed before [22,24,101–103]. In short, we use a knowledge-based Bayesian modeling approach as opposed to a more generally used data-driven approach, thus avoiding common problems with data-overfitting. This approach improves specificity in measuring signaling pathway activity, and enables development as a diagnostic assay across multiple disease types.

To explore the clinical utility of the biologically validated Notch pathway model, we have analyzed diagnostic samples from 117 pediatric T-ALL patients. We found that the Notch pathway activity score was related to the presence of NOTCH1-activating mutations and the type of mutations, and was correlated to the levels of ICN protein in these samples. Correspondingly, we found the highest Notch pathway activity scores in the TLX subgroup, a group that we described before as having the highest incidence of NOTCH1-activating mutations [35]. Most T-ALL patients in this T-ALL subgroup (21 out of 30 patients) bear *TLX3-BCL11B* rearrangements [98]. Moreover, the TLX subgroup is related to gamma-delta T-cell lineage development [104]. Interestingly, human gamma-delta T-cell lineage development especially depends on high Notch pathway activity levels, in contrast to alpha-beta T-lineage development [77]. The proliferative and TALLMO subgroups, which are associated with the early and late cortical stages of the alpha-beta T-lineage, respectively, indeed have lower Notch pathway activity scores. Therefore, the NOTCH dependency in normal development mirrors that of the respective T-ALL subgroups. Remarkably, about half of the ETP-ALL patients seem to have an activated Notch signaling pathway based on measured activity scores, despite their overall lower incidence of NOTCH-activating mutations [105]. We observed that various samples without, or with weak, NOTCH-activating mutations still have high Notch pathway activity scores [35]. This is especially evident for patients from the TLX subgroup, and points to other, as yet unidentified, mutations outside the present hotspot regions or other mechanisms that may activate the Notch pathway in T-ALL.

The patients with a Notch pathway activity score in the lowest 25th percentile had the worst event-free and relapse-free survival. Interestingly, NOTCH mutations in this cohort were not associated with beneficial outcomes, as reported before [35], while other studies identified activating NOTCH mutations as a favorable prognostic factor [37–39]. This result suggests that scoring the Notch pathway activity might be a more reliable method for determining prognosis than identifying NOTCH-activating mutations. In addition, the Notch pathway test has the potential to improve the stratification of patients to novel therapies targeting the Notch pathway.

The patients with the lowest Notch pathway activity scores were more likely to have functional PTEN loss, indicating that Notch pathway activation and PTEN inactivation reflect two distinct T-ALL entities, as we and others have reported before [100,106]. PTEN aberrancies are often found in the TALLMO T-ALL subgroup, in which they occur mutually exclusively with strong NOTCH1 mutations [100]. Moreover, patients with PTEN aberrancies have been shown to have an inferior survival rate [100,106]. The finding that PTEN aberrancies occurred more often in the patients with the lowest Notch pathway activity helps explain the inferior event-free/relapse-free survival of this group.

Overall, our results indicate that Notch pathway activity cannot be deduced from the presence of activating mutations only, which may provide an explanation for the differences in the prognostic significance of NOTCH-activating mutations in various pediatric and adult patient cohorts [36].

While the here-described Notch pathway assay is expected to be of value for a broad range of diseases, as well as for preclinical research and drug development, the first envisioned clinical application is therapy response prediction, e.g., to NOTCH inhibitors, for T-ALL, small cell lung cancer and other malignancies. To enable the use of the Notch pathway activity assay on formalin-fixed paraffin-embedded tissue samples, which are the standard in pathology diagnostics, the here-described Affymetrix-based Notch pathway activity test has been converted to an RT-qPCR-based test, which can be performed using standard lab equipment (in principle within three hours). To enable the determination of Notch pathway activity from RNA sequencing data, the assay has been converted to an RNAseq-based assay (www.philips.com/oncosignal). The conversion procedure has been described before, and does not involve the addition of new target genes [104,107]. These assays will be used in future clinical validation studies.

4. Materials and Methods

4.1. Development of the Notch Pathway Assay

The mathematical approach to developing Bayesian network models for the measurement of signal transduction pathway activity, based on mRNA expression analysis, has been described in detail before [24]. In brief, a causal computational network model for the Notch signal transduction pathway was generated that calculates the probability that NOTCH transcription factors are active, based on the expression levels of direct target genes (Figure 4). The Bayesian network describes the causal relation between the up- or downregulation of NOTCH target genes and the presence of an active or inactive NOTCH transcription complex. The parameters that describe this relationship are based on literature evidence, and are calibrated on patient samples with known Notch pathway activity. Target genes for the Notch pathway assay were selected according to the same principles as described before, using the available scientific literature [22,24]. The probesets of direct target genes from the publicly available Affymetrix (Santa Clara, CA, USA) HG-U133Plus2.0 microarray datasets were selected using the Bioconductor package, `hgu133plus2.db`, available in the statistical environment *R* and manually curated using GRCh38/hg38, available on the UCSC Genome Browser (www.genome.ucsc.edu, last access 9-30-2020) [26,28,32,108,109]. Probesets representing intronic sequences, probesets on opposite strands, and other chromosomal sequences than the respective target gene, were excluded. Probesets that were missing in Bioconductor were added.

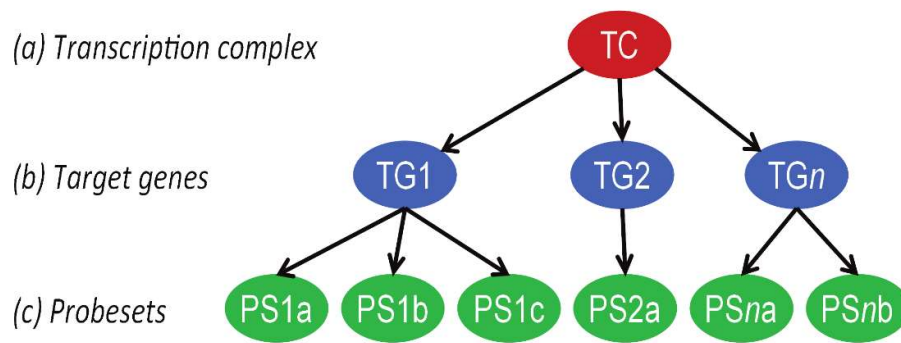


Figure 4. Bayesian model for the Notch signal transduction pathway. The structure of the Bayesian network used to model the transcriptional program of signaling pathways. The transcription complex refers to the transcription factor associated with a specific signal transduction pathway, which can be present in an inactive or active gene transcribing state; target genes refers to direct target genes of the transcription complex; probesets refers to probesets for the respective target gene present on Affymetrix HG-U133 Plus 2.0 microarray. With permission, [24].

4.2. Calibration and Validation of the Notch Pathway Activity Model

The Notch pathway Bayesian model, intended for generic use across different cell and tissue types, was calibrated on a single public dataset containing data from normal (low Notch pathway activity) and high-grade serous ovarian cancer (high Notch pathway activity) tissue samples [86]. Following calibration, the model parameters were frozen. Subsequently, given that the Bayesian model describes how expression and probeset measurements depend causally on pathway activity, it can be used to reason backwards from a set of given measurements to assess the likelihood that the pathway was active. Upon entering new mRNA probeset measurements into the model, this reasoning is performed by Bayesian inference, which yields the odds that the pathway is active vs. not, after which we apply a log2 transformation to obtain a symmetric scale with higher resolution at the extreme ends [22,23]. The resulting Notch pathway score reflects the amount of evidence delivered by the target gene expression levels for being active, and thus is a read-out of functional Notch signaling pathway activity. In general, higher target gene expression levels will lead to higher Notch activity, and vice versa. The model-based Notch pathway assay was validated using multiple independent Affymetrix datasets containing gene expression data from samples with known Notch pathway activity.

4.3. Microarray Data Source and Quality Control

The Affymetrix HG-U133Plus2.0 datasets used for Notch pathway model calibration and validation, and for the Notch pathway analysis of T-ALL (GSE26713), are available at the GEO website (www.ncbi.nlm.nih.gov/geo, last access 9-30-2020). GEO datasets have been listed with their associated publications in the figure legends. Before using the microarray data, extensive quality control was performed on the Affymetrix data from each individual sample, based on 12 different quality parameters according to Affymetrix's recommendations and previously published literature [22,110,111], and then they were further preprocessed in the statistical environment *R* using frozen RMA [112] with 'robust weighted average' summarization.

4.4. Description of the T-ALL Pediatric Patient Cohort

The Affymetrix HG-U133Plus2.0 gene expression profiles (GSE26713) from diagnostic biopsies of 117 T-ALL patients, who were treated according to the German co-operative study group for childhood ALL-97 protocol (COALL-97) or the Dutch Childhood Oncology Group (DCOG) protocols ALL-7,-8 or -9, were used in this study [98]. The patient data used in this study were obtained with informed consent from the subjects' guardians and in accordance with the Declaration of Helsinki.

4.5. Statistics

For the validations of the Notch pathway model, two-sided Wilcoxon signed-rank statistical tests were performed. Other used statistical methods that are more appropriate due to the content of a specific dataset are indicated in the figure legends. For pathway correlation statistics, both Pearson correlation and Spearman rank correlation tests were performed; since the results were similar, only the Pearson correlation coefficient and associated *p*-value are reported. For outcome analysis, Kaplan–Meier survival curves were calculated together with the associated *p*-value using the log-rank test.

4.6. Ethics Approval and Consent to Participate

Informed consent was given in accordance with the Institutional Review Board of the Erasmus MC Rotterdam and in accordance with the Declaration of Helsinki.

5. Conclusions

We have developed an assay to measure Notch pathway activity, which calculates a pathway activity score that is based on the expression levels of conserved Notch direct target genes. This assay was successfully validated by detecting the Notch activity in a variety of tumor models of different cellular origins with known Notch pathway activity, i.e., brain, lung, hematopoietic stem cells, and T-ALL cell lines. Our assay is expected to be of value for a broad range of diseases, as well as for preclinical research and drug development. The first envisioned clinical application is therapy response prediction, e.g., to NOTCH inhibitors, for T-ALL, small cell lung cancer and other malignancies.

Supplementary Materials: The following are available online at <http://www.mdpi.com/2072-6694/12/11/3142/s1>, Table S1: Scoring of NOTCH target genes with respect to evidence as to direct gene regulation by Notch transcription factors, Figure S1: Extended validation of the Notch pathway model in CUTLL1 cells, Figure S2: Correlations of ICN1 level and Notch pathway activity, divided per NOTCH1-activating mutation status.

Author Contributions: Conceptualization, W.V., A.v.d.S. and J.P.P.M.; Formal analysis, K.C.-B., L.H., R.H., V.C., A.v.d.S. and J.P.P.M.; Methodology, K.C.-B., L.H., H.v.O., W.V., A.v.d.S. and J.P.P.M.; Project administration, H.v.O. and J.P.P.M.; Supervision, A.v.d.S. and J.P.P.M.; Validation, L.H.; Visualization, K.C.-B., L.H. and R.H.; writing—original draft, K.C.-B., R.H., V.C. and A.v.d.S.; writing—review and editing, K.C.-B., L.H., A.v.d.S. and J.P.P.M. All authors have read and agreed to the published version of the manuscript.

Funding: K.C.-B and R.H. are funded by the Dutch ‘Kinderen Kanker Vrij’ foundation grants KiKa-295 and KiKa-219, respectively. V.C. is funded by the Dutch Cancer Society grant KWF-10355.

Conflicts of Interest: Laurent Holtzer, Henk van Ooijen, Wim Verhaegh, Anja van de Stolpe are employees of Royal Philips. The other authors declare no potential conflict of interest.

References

- Hanahan, D.; Weinberg, R.A. Hallmarks of cancer: The next generation. *Cell* **2011**, *144*, 646–674. [[CrossRef](#)]
- van de Stolpe, A.; Kauffmann, R.H. Innovative human-specific investigational approaches to autoimmune disease. *RSC Advances* **2015**, *5*, 18451–18463. [[CrossRef](#)]
- Marquart, J.; Chen, E.Y.; Prasad, V. Estimation of the Percentage of US Patients with Cancer Who Benefit From Genome-Driven Oncology. *JAMA Oncol.* **2018**, *4*, 1093–1098. [[CrossRef](#)] [[PubMed](#)]
- Massard, C.; Michiels, S.; Ferte, C.; Le Deley, M.C.; Lacroix, L.; Hollebecque, A.; Verlingue, L.; Ileana, E.; Rosellini, S.; Ammari, S.; et al. High-Throughput Genomics and Clinical Outcome in Hard-to-Treat Advanced Cancers: Results of the MOSCATO 01 Trial. *Cancer Discov.* **2017**, *7*, 586–595. [[CrossRef](#)] [[PubMed](#)]
- Deangelo, D.J.; Stone, R.M.; Silverman, L.B.; Stock, W.; Attar, E.C.; Fearen, I.; Dallob, A.; Matthews, C.; Stone, J.; Freedman, S.J.; et al. A phase I clinical trial of the notch inhibitor MK-0752 in patients with T-cell acute lymphoblastic leukemia/lymphoma (T-ALL) and other leukemias. *J. Clin. Oncol.* **2006**, *24*, 6585. [[CrossRef](#)]
- Roberts, K.G.; Li, Y.; Payne-Turner, D.; Harvey, R.C.; Yang, Y.L.; Pei, D.; McCastlain, K.; Ding, L.; Lu, C.; Song, G.; et al. Targetable kinase-activating lesions in Ph-like acute lymphoblastic leukemia. *N. Engl. J. Med.* **2014**, *371*, 1005–1015. [[CrossRef](#)] [[PubMed](#)]

7. Schultz, K.R.; Bowman, W.P.; Aledo, A.; Slayton, W.B.; Sather, H.; Devidas, M.; Wang, C.; Davies, S.M.; Gaynon, P.S.; Trigg, M.; et al. Improved early event-free survival with imatinib in Philadelphia chromosome-positive acute lymphoblastic leukemia: A children's oncology group study. *J. Clin. Oncol.* **2009**, *27*, 5175–5181. [[CrossRef](#)]
8. Arnal, J.F.; Lenfant, F.; Metivier, R.; Flouriot, G.; Henrion, D.; Adlanmerini, M.; Fontaine, C.; Gourdy, P.; Chambon, P.; Katzenellenbogen, B.; et al. Membrane and Nuclear Estrogen Receptor Alpha Actions: From Tissue Specificity to Medical Implications. *Physiol. Rev.* **2017**, *97*, 1045–1087. [[CrossRef](#)] [[PubMed](#)]
9. Burotto, M.; Chiou, V.L.; Lee, J.M.; Kohn, E.C. The MAPK pathway across different malignancies: A new perspective. *Cancer* **2014**, *120*, 3446–3456. [[CrossRef](#)]
10. Colak, S.; Ten Dijke, P. Targeting TGF-beta Signaling in Cancer. *Trends Cancer* **2017**, *3*, 56–71. [[CrossRef](#)]
11. Espin-Palazon, R.; Traver, D. The NF-kappaB family: Key players during embryonic development and HSC emergence. *Exp. Hematol.* **2016**, *44*, 519–527. [[CrossRef](#)] [[PubMed](#)]
12. Kono, M.; Fujii, T.; Lim, B.; Karuturi, M.S.; Tripathy, D.; Ueno, N.T. Androgen Receptor Function and Androgen Receptor-Targeted Therapies in Breast Cancer: A Review. *JAMA Oncol.* **2017**, *3*, 1266–1273. [[CrossRef](#)] [[PubMed](#)]
13. Lum, L.; Beachy, P.A. The Hedgehog response network: Sensors, switches, and routers. *Science* **2004**, *304*, 1755–1759. [[CrossRef](#)] [[PubMed](#)]
14. Massague, J. TGF-beta signal transduction. *Annu. Rev. Biochem.* **1998**, *67*, 753–791. [[CrossRef](#)] [[PubMed](#)]
15. Pardali, E.; Sanchez-Duffhues, G.; Gomez-Puerto, M.C.; Ten Dijke, P. TGF-beta-Induced Endothelial-Mesenchymal Transition in Fibrotic Diseases. *Int. J. Mol. Sci.* **2017**, *18*, 2157. [[CrossRef](#)]
16. Siebel, C.; Lendahl, U. Notch Signaling in Development, Tissue Homeostasis, and Disease. *Physiol. Rev.* **2017**, *97*, 1235–1294. [[CrossRef](#)] [[PubMed](#)]
17. Villarino, A.V.; Kanno, Y.; O'Shea, J.J. Mechanisms and consequences of Jak-STAT signaling in the immune system. *Nat. Immunol.* **2017**, *18*, 374–384. [[CrossRef](#)]
18. Chacon-Martinez, C.A.; Koester, J.; Wickstrom, S.A. Signaling in the stem cell niche: Regulating cell fate, function and plasticity. *Development* **2018**, *145*. [[CrossRef](#)]
19. Sanz-Ezquerro, J.J.; Munsterberg, A.E.; Stricker, S. Editorial: Signaling Pathways in Embryonic Development. *Front. Cell Dev. Biol.* **2017**, *5*, 76. [[CrossRef](#)]
20. Yu, J.S.; Cui, W. Proliferation, survival and metabolism: The role of PI3K/AKT/mTOR signalling in pluripotency and cell fate determination. *Development* **2016**, *143*, 3050–3060. [[CrossRef](#)]
21. Cantley, L.C.; Hunter, T.; Sever, R.; Thorner, J.W. *Signal. Transduction: Principles, Pathways, and Processes*; Cold Spring Harbor Laboratory Press: Cold Spring Harbor, NY, USA, 2014; ISBN 978-0-87969-901-7.
22. Stolpe, A.V.; Holtzer, L.; van Ooijen, H.; de Inda, M.A.; Verhaegh, W. Enabling precision medicine by unravelling disease pathophysiology: Quantifying signal transduction pathway activity across cell and tissue types. *Sci. Rep.* **2019**, *9*, 1603. [[CrossRef](#)] [[PubMed](#)]
23. van Ooijen, H.; Hornsveld, M.; Dam-de Veen, C.; Velter, R.; Dou, M.; Verhaegh, W.; Burgering, B.; van de Stolpe, A. Assessment of Functional Phosphatidylinositol 3-Kinase Pathway Activity in Cancer Tissue Using Forkhead Box-O Target Gene Expression in a Knowledge-Based Computational Model. *Am. J. Pathol.* **2018**, *188*, 1956–1972. [[CrossRef](#)]
24. Verhaegh, W.; van Ooijen, H.; Inda, M.A.; Hatzis, P.; Versteeg, R.; Smid, M.; Martens, J.; Foekens, J.; van de Wiel, P.; Clevers, H.; et al. Selection of personalized patient therapy through the use of knowledge-based computational models that identify tumor-driving signal transduction pathways. *Cancer Res.* **2014**, *74*, 2936–2945. [[CrossRef](#)] [[PubMed](#)]
25. Bouwman, W.; Verhaegh, W.; Holtzer, L.; van de Stolpe, A. Measurement of Cellular Immune Response to Viral Infection and Vaccination. *Front. Immunol.* **2020**, *11*. [[CrossRef](#)]
26. Locatelli, M.; Curigliano, G. Notch inhibitors and their role in the treatment of triple negative breast cancer: Promises and failures. *Curr. Opin. Oncol.* **2017**, *29*, 411–427. [[CrossRef](#)] [[PubMed](#)]
27. Milano, J.; McKay, J.; Dagenais, C.; Foster-Brown, L.; Pognan, F.; Gadiant, R.; Jacobs, R.T.; Zacco, A.; Greenberg, B.; Ciaccio, P.J. Modulation of notch processing by gamma-secretase inhibitors causes intestinal goblet cell metaplasia and induction of genes known to specify gut secretory lineage differentiation. *Toxicol. Sci.* **2004**, *82*, 341–358. [[CrossRef](#)] [[PubMed](#)]

28. Real, P.J.; Tosello, V.; Palomero, T.; Castillo, M.; Hernando, E.; de Stanchina, E.; Sulis, M.L.; Barnes, K.; Sawai, C.; Homminga, I.; et al. Gamma-secretase inhibitors reverse glucocorticoid resistance in T cell acute lymphoblastic leukemia. *Nat. Med.* **2009**, *15*, 50–58. [[CrossRef](#)] [[PubMed](#)]
29. Searfoss, G.H.; Jordan, W.H.; Calligaro, D.O.; Galbreath, E.J.; Schirtzinger, L.M.; Berridge, B.R.; Gao, H.; Higgins, M.A.; May, P.C.; Ryan, T.P. Adipsin, a biomarker of gastrointestinal toxicity mediated by a functional gamma-secretase inhibitor. *J. Biol. Chem.* **2003**, *278*, 46107–46116. [[CrossRef](#)]
30. van Es, J.H.; van Gijn, M.E.; Riccio, O.; van den Born, M.; Vooijs, M.; Begthel, H.; Cozijnsen, M.; Robine, S.; Winton, D.J.; Radtke, F.; et al. Notch/gamma-secretase inhibition turns proliferative cells in intestinal crypts and adenomas into goblet cells. *Nature* **2005**, *435*, 959–963. [[CrossRef](#)]
31. Wong, G.T.; Manfra, D.; Poulet, F.M.; Zhang, Q.; Josien, H.; Bara, T.; Engstrom, L.; Pinzon-Ortiz, M.; Fine, J.S.; Lee, H.J.; et al. Chronic treatment with the gamma-secretase inhibitor LY-411,575 inhibits beta-amyloid peptide production and alters lymphopoiesis and intestinal cell differentiation. *J. Biol. Chem.* **2004**, *279*, 12876–12882. [[CrossRef](#)]
32. Li, D.; Masiero, M.; Banham, A.H.; Harris, A.L. The notch ligand JAGGED1 as a target for anti-tumor therapy. *Front. Oncol.* **2014**, *4*, 254. [[CrossRef](#)] [[PubMed](#)]
33. Lehman, J.M.; Horn, L. Targeted therapy in small cell lung cancer: Can DLL3 notch up a victory? *Transl. Cancer Res.* **2017**, *6*, S453–S456. [[CrossRef](#)]
34. Weng, A.P.; Ferrando, A.A.; Lee, W.; Morris, J.P.; Silverman, L.B.; Sanchez-Irizarry, C.; Blacklow, S.C.; Look, A.T.; Aster, J.C. Activating mutations of NOTCH1 in human T cell acute lymphoblastic leukemia. *Science* **2004**, *306*, 269–271. [[CrossRef](#)]
35. Zuurbier, L.; Homminga, I.; Calvert, V.; te Winkel, M.L.; Buijs-Gladdines, J.G.; Kooi, C.; Smits, W.K.; Sonneveld, E.; Veerman, A.J.; Kamps, W.A.; et al. NOTCH1 and/or FBXW7 mutations predict for initial good prednisone response but not for improved outcome in pediatric T-cell acute lymphoblastic leukemia patients treated on DCOG or COALL protocols. *Leukemia* **2010**, *24*, 2014–2022. [[CrossRef](#)] [[PubMed](#)]
36. Hefazi, M.; Litzow, M.R. Recent Advances in the Biology and Treatment of T Cell Acute Lymphoblastic Leukemia. *Curr. Hematol. Malign Rep.* **2018**, *13*, 265–274. [[CrossRef](#)] [[PubMed](#)]
37. Breit, S.; Stanulla, M.; Flohr, T.; Schrappe, M.; Ludwig, W.D.; Tolle, G.; Happich, M.; Muckenthaler, M.U.; Kulozik, A.E. Activating NOTCH1 mutations predict favorable early treatment response and long-term outcome in childhood precursor T-cell lymphoblastic leukemia. *Blood* **2006**, *108*, 1151–1157. [[CrossRef](#)] [[PubMed](#)]
38. Clappier, E.; Collette, S.; Grardel, N.; Girard, S.; Suarez, L.; Brunie, G.; Kaltenbach, S.; Yakouben, K.; Mazingue, F.; Robert, A.; et al. NOTCH1 and FBXW7 mutations have a favorable impact on early response to treatment, but not on outcome, in children with T-cell acute lymphoblastic leukemia (T-ALL) treated on EORTC trials 58881 and 58951. *Leukemia* **2010**, *24*, 2023–2031. [[CrossRef](#)] [[PubMed](#)]
39. Kox, C.; Zimmermann, M.; Stanulla, M.; Leible, S.; Schrappe, M.; Ludwig, W.D.; Koehler, R.; Tolle, G.; Bandapalli, O.R.; Breit, S.; et al. The favorable effect of activating NOTCH1 receptor mutations on long-term outcome in T-ALL patients treated on the ALL-BFM 2000 protocol can be separated from FBXW7 loss of function. *Leukemia* **2010**, *24*, 2005–2013. [[CrossRef](#)]
40. Alaña, L.; Sesé, M.; Cánovas, V.; Punyal, Y.; Fernández, Y.; Abasolo, I.; de Torres, I.; Ruiz, C.; Espinosa, L.; Bigas, A.; et al. Prostate tumor Overexpressed-1 (PTOV1) down-regulates HES1 and HEY1 notch targets genes and promotes prostate cancer progression. *Mol. Cancer* **2014**, *13*, 74. [[CrossRef](#)]
41. Bessho, Y.; Miyoshi, G.; Sakata, R.; Kageyama, R. Hes7: A bHLH-type repressor gene regulated by Notch and expressed in the presomitic mesoderm. *Genes Cells* **2001**, *6*, 175–185. [[CrossRef](#)]
42. Chen, X.; Thiaville, M.M.; Chen, L.; Stoeck, A.; Xuan, J.; Gao, M.; Shih, I.-M.; Wang, T.-L. Defining NOTCH3 target genes in ovarian cancer. *Cancer Res.* **2012**, *72*, 2294–2303. [[CrossRef](#)] [[PubMed](#)]
43. de la Pompa, J.L.; Wakeham, A.; Correia, K.M.; Samper, E.; Brown, S.; Aguilera, R.J.; Nakano, T.; Honjo, T.; Mak, T.W.; Rossant, J.; et al. Conservation of the Notch signalling pathway in mammalian neurogenesis. *Development* **1997**, *124*, 1139–1148. [[PubMed](#)]
44. Deftos, M.L.; He, Y.-W.; Ojala, E.W.; Bevan, M.J. Correlating Notch Signaling with Thymocyte Maturation. *Immunity* **1998**, *9*, 777–786. [[CrossRef](#)]
45. Diaz-Cuadros, M.; Wagner, D.E.; Budjan, C.; Hubaud, A.; Tarazona, O.A.; Donnelly, S.; Michaut, A.; Al Tanoury, Z.; Yoshioka-Kobayashi, K.; Niino, Y.; et al. In vitro characterization of the human segmentation clock. *Nature* **2020**, *580*, 113–118. [[CrossRef](#)] [[PubMed](#)]

46. Hamidi, H.; Gustafason, D.; Pellegrini, M.; Gasson, J. Identification of novel targets of CSL-dependent Notch signaling in hematopoiesis. *PLoS ONE* **2011**, *6*, e20022. [[CrossRef](#)]
47. Iso, T.; Chung, G.; Hamamori, Y.; Kedes, L. HERP1 is a cell type-specific primary target of Notch. *J. Biol. Chem.* **2001**, *277*, 6598–6607. [[CrossRef](#)]
48. Iso, T.; Sartorelli, V.; Chung, G.; Shichinohe, T.; Kedes, L.; Hamamori, Y. HERP, a new primary target of Notch regulated by ligand binding. *Mol. Cell. Biol.* **2001**, *21*, 6071–6079. [[CrossRef](#)]
49. Jäggle, S.; Rönsch, K.; Timme, S.; Andrlová, H.; Bertrand, M.; Jäger, M.; Proske, A.; Schrempp, M.; Yousaf, A.; Michoel, T.; et al. Silencing of the EPHB3 tumor-suppressor gene in human colorectal cancer through decommissioning of a transcriptional enhancer. *Proc. Natl. Acad. Sci. USA* **2014**, *111*, 4886–4891. [[CrossRef](#)]
50. Jarriault, S.; Brou, C.; Logeat, F.; Schroeter, E.H.; Kopan, R.; Israel, A. Signalling downstream of activated mammalian Notch. *Nature* **1995**, *377*, 355–358. [[CrossRef](#)]
51. Katoh, M.; Katoh, M. Integrative genomic analyses on HES/HEY family: Notch-independent HES1, HES3 transcription in undifferentiated ES cells, and Notch-dependent HES1, HES5, HEY1, HEY2, HEYL transcription in fetal tissues, adult tissues, or cancer. *Int. J. Oncol.* **2007**, *31*, 461–466. [[CrossRef](#)]
52. Kim, H.; Huang, L.; Critser, P.J.; Yang, Z.; Chan, R.J.; Wang, L.; Carlesso, N.; Voytik-Harbin, S.L.; Bernstein, I.D.; Yoder, M.C. Notch ligand Delta-like 1 promotes in vivo vasculogenesis in human cord blood-derived endothelial colony forming cells. *Cytotherapy* **2015**, *17*, 579–592. [[CrossRef](#)] [[PubMed](#)]
53. Krebs, L.T.; Deftos, M.L.; Bevan, M.J.; Gridley, T. The Nrarp gene encodes an ankyrin-repeat protein that is transcriptionally regulated by the notch signaling pathway. *Dev. Biol.* **2002**, *238*, 110–119. [[CrossRef](#)] [[PubMed](#)]
54. Kulic, I.; Robertson, G.; Chang, L.; Baker, J.H.E.; Lockwood, W.W.; Mok, W.; Fuller, M.; Fournier, M.; Wong, N.; Chou, V.; et al. Loss of the Notch effector RBPJ promotes tumorigenesis. *J. Exp. Med.* **2014**, *212*, 37–52. [[CrossRef](#)]
55. Kulsum, S.; Raju, N.; Raghavan, N.; Ramanjanappa, R.D.R.; Sharma, A.; Mehta, A.; Kuriakose, M.A.; Suresh, A. Cancer stem cells and fibroblast niche cross talk in an in-vitro oral dysplasia model. *Mol. Carcinog.* **2019**, *58*, 820–831. [[CrossRef](#)]
56. Kuroda, K.; Tani, S.; Tamura, K.; Minoguchi, S.; Kurooka, H.; Honjo, T. Delta-induced Notch signaling mediated by RBP-J inhibits MyoD expression and myogenesis. *J. Biol. Chem.* **1999**, *274*, 7238–7244. [[CrossRef](#)]
57. Leimeister, C.; Schumacher, N.; Steidl, C.; Gessler, M. Analysis of HeyL expression in wild-type and Notch pathway mutant mouse embryos. *Mech. Dev.* **2000**, *98*, 175–178. [[CrossRef](#)]
58. Li, G.-H.; Fan, Y.-Z.; Liu, X.-W.; Zhang, B.-F.; Yin, D.-D.; He, F.; Huang, S.-Y.; Kang, Z.-J.; Xu, H.; Liu, Q.; et al. Notch signaling maintains proliferation and survival of the HL60 human promyelocytic leukemia cell line and promotes the phosphorylation of the Rb protein. *Mol. Cell. Biochem.* **2010**, *340*, 7–14. [[CrossRef](#)]
59. Li, Y.; Hibbs, M.A.; Gard, A.L.; Shylo, N.A.; Yun, K. Genome-wide analysis of N1ICD/RBPJ targets in vivo reveals direct transcriptional regulation of Wnt, SHH, and hippo pathway effectors by Notch1. *STEM CELLS* **2012**, *30*, 741–752. [[CrossRef](#)] [[PubMed](#)]
60. Liao, W.-R.; Hsieh, R.-H.; Hsu, K.-W.; Wu, M.-Z.; Tseng, M.-J.; Mai, R.-T.; Lee, Y.-H.W.; Yeh, T.-S. The CBF1-independent Notch1 signal pathway activates human c-myc expression partially via transcription factor YY1. *Carcinogenesis* **2007**, *28*, 1867–1876. [[CrossRef](#)]
61. Magnani, L.; Stoeck, A.; Zhang, X.; Lánczky, A.; Mirabella, A.C.; Wang, T.-L.; Györfy, B.; Lupien, M. Genome-wide reprogramming of the chromatin landscape underlies endocrine therapy resistance in breast cancer. *Pro. Natl. Acad. Sci. USA* **2013**, *110*, E1490–E1499. [[CrossRef](#)] [[PubMed](#)]
62. Maier, M.M.; Gessler, M. Comparative analysis of the human and mouse Hey1 promoter: Hey genes are new Notch target genes. *Biochem. Biophys. Res. Commun.* **2000**, *275*, 652–660. [[CrossRef](#)] [[PubMed](#)]
63. Martini, S.; Bernoth, K.; Main, H.; Ortega, G.D.C.; Lendahl, U.; Just, U.; Schwanbeck, R. A critical role for Sox9 in notch-induced astroglialogenesis and stem cell maintenance. *STEM CELLS* **2013**, *31*, 741–751. [[CrossRef](#)] [[PubMed](#)]
64. Meier-Stiegen, F.; Schwanbeck, R.; Bernoth, K.; Martini, S.; Hieronymus, T.; Ruau, D.; Zenke, M.; Just, U. Activated Notch1 target genes during embryonic cell differentiation depend on the cellular context and include lineage determinants and inhibitors. *PLoS ONE* **2010**, *5*, e11481. [[CrossRef](#)] [[PubMed](#)]
65. Oswald, F.; Liptay, S.; Adler, G.; Schmid, R.M. NF-kappaB2 is a putative target gene of activated Notch-1 via RBP-Jkappa. *Mol. Cell. Biol.* **1998**, *18*, 2077–2088. [[CrossRef](#)] [[PubMed](#)]

66. Palomero, T.; Barnes, K.C.; Real, P.J.; Bender, J.L.G.; Sulis, M.L.; Murty, V.V.; Colovai, A.I.; Balbin, M.; Ferrando, A.A. CUTLL1, a novel human T-cell lymphoma cell line with t(7;9) rearrangement, aberrant NOTCH1 activation and high sensitivity to gamma-secretase inhibitors. *Leukemia* **2006**, *20*, 1279–1287. [[CrossRef](#)] [[PubMed](#)]
67. Palomero, T.; Lim, W.K.; Odom, D.T.; Sulis, M.L.; Real, P.J.; Margolin, A.; Barnes, K.C.; O’Neil, J.; Neuberg, D.; Weng, A.P.; et al. NOTCH1 directly regulates c-MYC and activates a feed-forward-loop transcriptional network promoting leukemic cell growth. *Proc. Natl. Acad. Sci. USA* **2006**, *103*, 18261–18266. [[CrossRef](#)]
68. Park, J.T.; Shih, I.-M.; Wang, T.-L. Identification of Pbx1, a potential oncogene, as a Notch3 target gene in ovarian cancer. *Cancer Res.* **2008**, *68*, 8852–8860. [[CrossRef](#)]
69. Pirot, P.; van Grunsven, L.A.; Marine, J.-C.; Huylebroeck, D.; Bellefroid, E.J. Direct regulation of the Nrarp gene promoter by the Notch signaling pathway. *Biochem. Biophys. Res. Commun.* **2004**, *322*, 526–534. [[CrossRef](#)]
70. Rad, E.B.; Hammerlindl, H.; Wels, C.; Popper, U.; Menon, D.R.; Breiteneder, H.; Kitzwoegerer, M.; Hafner, C.; Herlyn, M.; Bergler, H.; et al. Notch4 Signaling Induces a Mesenchymal-Epithelial-like Transition in Melanoma Cells to Suppress Malignant Behaviors. *Cancer Res.* **2016**, *76*, 1690–1697.
71. Rehman, M.; Gurrapu, S.; Cagnoni, G.; Capparruccia, L.; Tamagnone, L. PlexinD1 Is a Novel Transcriptional Target and Effector of Notch Signaling in Cancer Cells. *PLoS ONE* **2016**, *11*, e0164660. [[CrossRef](#)]
72. Rodilla, V.; Villanueva, A.; Obrador-Hevia, A.; Robert-Moreno, A.; Fernandez-Majada, V.; Grilli, A.; Lopez-Bigas, N.; Bellora, N.; Alba, M.M.; Torres, F.; et al. Jagged1 is the pathological link between Wnt and Notch pathways in colorectal cancer. *Proc. Natl. Acad. Sci. USA* **2009**, *106*, 6315–6320. [[CrossRef](#)] [[PubMed](#)]
73. Rustighi, A.; Tiberi, L.; Soldano, A.; Napoli, M.; Nuciforo, P.; Rosato, A.; Kaplan, F.; Capobianco, A.; Pece, S.; Di Fiore, P.P.; et al. The prolyl-isomerase Pin1 is a Notch1 target that enhances Notch1 activation in cancer. *Nat. Cell Biol.* **2009**, *11*, 133–142. [[CrossRef](#)]
74. Schroeter, E.H.; Kisslinger, J.A.; Kopan, R. Notch-1 signalling requires ligand-induced proteolytic release of intracellular domain. *Nature* **1998**, *393*, 382–386. [[CrossRef](#)]
75. Sharma, V.M.; Calvo, J.A.; Draheim, K.M.; Cunningham, L.A.; Hermance, N.; Beverly, L.; Krishnamoorthy, V.; Bhasin, M.; Capobianco, A.J.; Kelliher, M.A. Notch1 contributes to mouse T-cell leukemia by directly inducing the expression of c-myc. *Mol. Cell. Biol.* **2006**, *26*, 8022–8031. [[CrossRef](#)]
76. Stoeck, A.; Lejnine, S.; Truong, A.; Pan, L.; Wang, H.; Zang, C.; Yuan, J.; Ware, C.; MacLean, J.; Garrett-Engele, P.W.; et al. Discovery of Biomarkers Predictive of GSI Response in Triple-Negative Breast Cancer and Adenoid Cystic Carcinoma. *Cancer Dis.* **2014**, *4*, 1154. [[CrossRef](#)]
77. Van de Walle, I.; De Smet, G.; De Smedt, M.; Vandekerckhove, B.; Leclercq, G.; Plum, J.; Taghon, T. An early decrease in Notch activation is required for human TCR-alpha-beta lineage differentiation at the expense of TCR-gammadelta T cells. *Blood* **2009**, *113*, 2988–2998. [[CrossRef](#)] [[PubMed](#)]
78. Vilimas, T.; Mascarenhas, J.; Palomero, T.; Mandal, M.; Buonamici, S.; Meng, F.; Thompson, B.; Spaulding, C.; Macaroun, S.; Alegre, M.-L.; et al. Targeting the NF-kappaB signaling pathway in Notch1-induced T-cell leukemia. *Nat. Med.* **2006**, *13*, 70–77. [[CrossRef](#)] [[PubMed](#)]
79. Weng, A.P.; Millholland, J.M.; Yashiro-Ohtani, Y.; Arcangeli, M.L.; Lau, A.; Wai, C.; Del Bianco, C.; Rodriguez, C.G.; Sai, H.; Tobias, J.; et al. c-Myc is an important direct target of Notch1 in T-cell acute lymphoblastic leukemia/lymphoma. *Genes Dev.* **2006**, *20*, 2096–2109. [[CrossRef](#)]
80. Xiao, Y.; Ye, Y.; Zou, X.; Jones, S.; Yearsley, K.; Shetuni, B.; Tellez, J.; Barsky, S.H. The lymphovascular embolus of inflammatory breast cancer exhibits a Notch 3 addiction. *Oncogene* **2010**, *30*, 287–300. [[CrossRef](#)] [[PubMed](#)]
81. Zong, Y.; Panikkar, A.; Xu, J.; Antoniou, A.; Raynaud, P.; Lemaigre, F.; Stanger, B.Z. Notch signaling controls liver development by regulating biliary differentiation. *Development* **2009**, *136*, 1727–1739. [[CrossRef](#)]
82. Wang, H.; Zou, J.; Zhao, B.; Johannsen, E.; Ashworth, T.; Wong, H.; Pear, W.S.; Schug, J.; Blacklow, S.C.; Arnett, K.L.; et al. Genome-wide analysis reveals conserved and divergent features of Notch1/RBPJ binding in human and murine T-lymphoblastic leukemia cells. *Proc. Natl. Acad. Sci. USA* **2011**, *108*, 14908–14913. [[CrossRef](#)] [[PubMed](#)]
83. Groeneweg, J.W.; Foster, R.; Growdon, W.B.; Verheijen, R.H.; Rueda, B.R. Notch signaling in serous ovarian cancer. *J. Ovarian Res.* **2014**, *7*, 95. [[CrossRef](#)] [[PubMed](#)]
84. Hu, W.; Liu, T.; Ivan, C.; Sun, Y.; Huang, J.; Mangala, L.S.; Miyake, T.; Dalton, H.J.; Pradeep, S.; Rupaimoole, R.; et al. Notch3 pathway alterations in ovarian cancer. *Cancer Res.* **2014**, *74*, 3282–3293. [[CrossRef](#)] [[PubMed](#)]

85. Park, J.T.; Li, M.; Nakayama, K.; Mao, T.L.; Davidson, B.; Zhang, Z.; Kurman, R.J.; Eberhart, C.G.; Shih, Ie, M.; Wang, T.L. Notch3 gene amplification in ovarian cancer. *Cancer Res.* **2006**, *66*, 6312–6318. [[CrossRef](#)] [[PubMed](#)]
86. Cancer Genome Atlas Research, N. Integrated genomic analyses of ovarian carcinoma. *Nature* **2011**, *474*, 609–615. [[CrossRef](#)] [[PubMed](#)]
87. Parcelier, A.; Maharzi, N.; Delord, M.; Robledo-Sarmiento, M.; Nelson, E.; Belakhdar-Mekid, H.; Pla, M.; Kuranda, K.; Parietti, V.; Goodhardt, M.; et al. AF1q/MLLT11 regulates the emergence of human prothymocytes through cooperative interaction with the Notch signaling pathway. *Blood* **2011**, *118*, 1784–1796. [[CrossRef](#)]
88. Tse, W.; Zhu, W.; Chen, H.S.; Cohen, A. A novel gene, AF1q, fused to MLL in t(1;11) (q21;q23), is specifically expressed in leukemic and immature hematopoietic cells. *Blood* **1995**, *85*, 650–656. [[CrossRef](#)]
89. Kridel, R.; Meissner, B.; Rogic, S.; Boyle, M.; Telenius, A.; Woolcock, B.; Gunawardana, J.; Jenkins, C.; Cochrane, C.; Ben-Neriah, S.; et al. Whole transcriptome sequencing reveals recurrent NOTCH1 mutations in mantle cell lymphoma. *Blood* **2012**, *119*, 1963–1971. [[CrossRef](#)]
90. Mok, S.C.; Bonome, T.; Vathipadiekal, V.; Bell, A.; Johnson, M.E.; Wong, K.K.; Park, D.C.; Hao, K.; Yip, D.K.; Donninger, H.; et al. A gene signature predictive for outcome in advanced ovarian cancer identifies a survival factor: Microfibril-associated glycoprotein 2. *Cancer Cell* **2009**, *16*, 521–532. [[CrossRef](#)]
91. Stany, M.P.; Vathipadiekal, V.; Ozbun, L.; Stone, R.L.; Mok, S.C.; Xue, H.; Kagami, T.; Wang, Y.; McAlpine, J.N.; Bowtell, D.; et al. Identification of novel therapeutic targets in microdissected clear cell ovarian cancers. *PLoS ONE* **2011**, *6*, e21121. [[CrossRef](#)]
92. Elgaaen, B.V.; Olstad, O.K.; Sandvik, L.; Odegaard, E.; Sauer, T.; Staff, A.C.; Gautvik, K.M. ZNF385B and VEGFA are strongly differentially expressed in serous ovarian carcinomas and correlate with survival. *PLoS ONE* **2012**, *7*, e46317. [[CrossRef](#)] [[PubMed](#)]
93. Tothill, R.W.; Tinker, A.V.; George, J.; Brown, R.; Fox, S.B.; Lade, S.; Johnson, D.S.; Trivett, M.K.; Etemadmoghadam, D.; Locandro, B.; et al. Novel molecular subtypes of serous and endometrioid ovarian cancer linked to clinical outcome. *Clin. Cancer Res.* **2008**, *14*, 5198–5208. [[CrossRef](#)] [[PubMed](#)]
94. van Nes, J.; Chan, A.; van Groningen, T.; van Sluis, P.; Koster, J.; Versteeg, R. A NOTCH3 transcriptional module induces cell motility in neuroblastoma. *Clin. Cancer Res.* **2013**, *19*, 3485–3494. [[CrossRef](#)] [[PubMed](#)]
95. Luistro, L.; He, W.; Smith, M.; Packman, K.; Vilenchik, M.; Carvajal, D.; Roberts, J.; Cai, J.; Berkofsky-Fessler, W.; Hilton, H.; et al. Preclinical profile of a potent gamma-secretase inhibitor targeting notch signaling with in vivo efficacy and pharmacodynamic properties. *Cancer Res.* **2009**, *69*, 7672–7680. [[CrossRef](#)] [[PubMed](#)]
96. Samon, J.B.; Castillo-Martin, M.; Hadler, M.; Ambesi-Impio, A.; Paietta, E.; Racevskis, J.; Wiernik, P.H.; Rowe, J.M.; Jakubczak, J.; Randolph, S.; et al. Preclinical analysis of the gamma-secretase inhibitor PF-03084014 in combination with glucocorticoids in T-cell acute lymphoblastic leukemia. *Mol. Cancer Ther.* **2012**, *11*, 1565–1575. [[CrossRef](#)]
97. Dohda, T.; Maljukova, A.; Liu, L.; Heyman, M.; Grander, D.; Brodin, D.; Sangfelt, O.; Lendahl, U. Notch signaling induces SKP2 expression and promotes reduction of p27Kip1 in T-cell acute lymphoblastic leukemia cell lines. *Exp. Cell Res.* **2007**, *313*, 3141–3152. [[CrossRef](#)]
98. Homminga, I.; Pieters, R.; Langerak, A.W.; de Rooij, J.J.; Stubbs, A.; Verstegen, M.; Vuerhard, M.; Buijs-Gladdines, J.; Kooi, C.; Klous, P.; et al. Integrated transcript and genome analyses reveal NKX2-1 and MEF2C as potential oncogenes in T cell acute lymphoblastic leukemia. *Cancer Cell* **2011**, *19*, 484–497. [[CrossRef](#)]
99. Chiang, M.Y.; Xu, L.; Shestova, O.; Histen, G.; L’Heureux, S.; Romany, C.; Childs, M.E.; Gimotty, P.A.; Aster, J.C.; Pear, W.S. Leukemia-associated NOTCH1 alleles are weak tumor initiators but accelerate K-ras-initiated leukemia. *J. Clin. Invest.* **2008**, *118*, 3181–3194. [[CrossRef](#)]
100. Zuurbier, L.; Petricoin, E.F., 3rd; Vuerhard, M.J.; Calvert, V.; Kooi, C.; Buijs-Gladdines, J.G.; Smits, W.K.; Sonneveld, E.; Veerman, A.J.; Kamps, W.A.; et al. The significance of PTEN and AKT aberrations in pediatric T-cell acute lymphoblastic leukemia. *Haematologica* **2012**, *97*, 1405–1413. [[CrossRef](#)]
101. Huang da, W.; Sherman, B.T.; Lempicki, R.A. Systematic and integrative analysis of large gene lists using DAVID bioinformatics resources. *Nat. Protoc.* **2009**, *4*, 44–57. [[CrossRef](#)]
102. Subramanian, A.; Tamayo, P.; Mootha, V.K.; Mukherjee, S.; Ebert, B.L.; Gillette, M.A.; Paulovich, A.; Pomeroy, S.L.; Golub, T.R.; Lander, E.S.; et al. Gene set enrichment analysis: A knowledge-based approach for interpreting genome-wide expression profiles. *Proc. Natl. Acad. Sci. USA* **2005**, *102*, 15545–15550. [[CrossRef](#)]

103. van de Stolpe, A. Quantitative Measurement of Functional Activity of the PI3K Signaling Pathway in Cancer. *Cancers* **2019**, *11*, 293. [[CrossRef](#)] [[PubMed](#)]
104. van Grotel, M.; Meijerink, J.P.; van Wering, E.R.; Langerak, A.W.; Beverloo, H.B.; Buijs-Gladdines, J.G.; Burger, N.B.; Passier, M.; van Lieshout, E.M.; Kamps, W.A.; et al. Prognostic significance of molecular-cytogenetic abnormalities in pediatric T-ALL is not explained by immunophenotypic differences. *Leukemia* **2008**, *22*, 124–131. [[CrossRef](#)] [[PubMed](#)]
105. Zhang, J.; Ding, L.; Holmfeldt, L.; Wu, G.; Heatley, S.L.; Payne-Turner, D.; Easton, J.; Chen, X.; Wang, J.; Rusch, M.; et al. The genetic basis of early T-cell precursor acute lymphoblastic leukaemia. *Nature* **2012**, *481*, 157–163. [[CrossRef](#)]
106. Trinquand, A.; Tanguy-Schmidt, A.; Ben Abdelali, R.; Lambert, J.; Beldjord, K.; Lengline, E.; De Gunzburg, N.; Payet-Bornet, D.; Lhermitte, L.; Mossafa, H.; et al. Toward a NOTCH1/FBXW7/RAS/PTEN-based oncogenetic risk classification of adult T-cell acute lymphoblastic leukemia: A Group for Research in Adult Acute Lymphoblastic Leukemia study. *J. Clin. Oncol.* **2013**, *31*, 4333–4342. [[CrossRef](#)]
107. Inda, M.A.; Blok, E.J.; Kuppen, P.J.K.; Charehbili, A.; den Biezen-Timmermans, E.C.; van Brussel, A.; Fruytier, S.E.; Meershoek-Klein Kranenbarg, E.; Kloet, S.; van der Burg, B.; et al. Estrogen Receptor Pathway Activity Score to Predict Clinical Response or Resistance to Neoadjuvant Endocrine Therapy in Primary Breast Cancer. *Mol. Cancer Ther.* **2020**, *19*, 680–689. [[CrossRef](#)]
108. Endres, K.; Deller, T. Regulation of Alpha-Secretase ADAM10 In vitro and In vivo: Genetic, Epigenetic, and Protein-Based Mechanisms. *Front. Mol. Neurosci.* **2017**, *10*, 56. [[CrossRef](#)]
109. Sanchez-Martin, M.; Ambesi-Impiombato, A.; Qin, Y.; Herranz, D.; Bansal, M.; Girardi, T.; Paietta, E.; Tallman, M.S.; Rowe, J.M.; De Keersmaecker, K.; et al. Synergistic antileukemic therapies in NOTCH1-induced T-ALL. *Proc. Natl. Acad. Sci. USA* **2017**, *114*, 2006–2011. [[CrossRef](#)]
110. Heber, S.; Sick, B. Quality assessment of Affymetrix GeneChip data. *OMICS* **2006**, *10*, 358–368. [[CrossRef](#)] [[PubMed](#)]
111. Wilson, C.L.; Miller, C.J. Simpleaffy: A BioConductor package for Affymetrix Quality Control and data analysis. *Bioinformatics* **2005**, *21*, 3683–3685. [[CrossRef](#)]
112. McCall, M.N.; Bolstad, B.M.; Irizarry, R.A. Frozen robust multiarray analysis (fRMA). *Biostatistics* **2010**, *11*, 242–253. [[CrossRef](#)] [[PubMed](#)]

Publisher’s Note: MDPI stays neutral with regard to jurisdictional claims in published maps and institutional affiliations.



© 2020 by the authors. Licensee MDPI, Basel, Switzerland. This article is an open access article distributed under the terms and conditions of the Creative Commons Attribution (CC BY) license (<http://creativecommons.org/licenses/by/4.0/>).